

Synthesis of LLDPE/TiO₂ nanocomposites by *in situ* polymerization with zirconocene/dMMAO catalyst: effect of [Al]/[Zr] ratios and TiO₂ phases

Wathanyoo Owpradit · Okorn Mekasuwandumrong ·
Joongjai Panpranot · Artiwan Shotipruk ·
Bunjerd Jongsomjit

Received: 7 January 2010 / Revised: 17 March 2010 / Accepted: 2 May 2010 /

Published online: 7 May 2010

© Springer-Verlag 2010

Abstract This article reveals the dependence of crystalline phases in titania on the intrinsic activity during *in situ* polymerization of ethylene/1-hexene using the zirconocene/dMMAO catalyst to produce LLDPE/TiO₂ nanocomposites. First, the TiO₂ nanoparticles having different crystalline phases were employed as the nanofillers by impregnation with dMMAO to obtain dMMAO/TiO₂. Then, copolymerization of ethylene/1-hexene using zirconocene catalyst was performed in the presence of dMMAO/TiO₂. It was found that the catalytic activity derived from the anatase TiO₂ (A) was about four times higher than that obtained from the rutile TiO₂ (R). This was likely due to higher intrinsic activity of the active species present on the TiO₂ (A). In addition, increased [Al]_{dMMAO}/[Zr]_{cat} ratios apparently resulted in enhanced activities for both TiO₂ (A) and TiO₂ (R). However, the TiO₂ (R) showed less deactivation upon increased [Al]_{dMMAO}/[Zr]_{cat} ratios. This can be attributed to strong interaction between dMMAO and TiO₂ (R) as proven by the TGA measurement. The microstructure of the LLDPE/TiO₂ obtained was found to be random copolymer for both TiO₂ (A) and TiO₂ (R).

Keywords Zirconocene catalyst · Cocatalyst · Catalyst characterization · Polymer nanocomposite · Titania

W. Owpradit · J. Panpranot · A. Shotipruk · B. Jongsomjit (✉)

Faculty of Engineering, Department of Chemical Engineering, Center of Excellence on Catalysis and Catalytic Reaction Engineering, Chulalongkorn University, Bangkok 10330, Thailand
e-mail: bunjerd.j@chula.ac.th

O. Mekasuwandumrong

Faculty of Engineering and Industrial Technology, Silapakorn University, Nakhonprathom 26000, Thailand

Introduction

The metallocene catalysts can be commercially used for the synthesis of specialty polymers with different structures and properties. In fact, the metallocenes are crucial, especially for olefin polymerization because they can control the properties of polyolefins. Metallocene catalysts are often used in the heterogeneous form based on the most existent technologies, such as gas phase and slurry polymerization. Hence, they are needed to support on inorganic carriers prior to polymerization. The reasons for the heterogenization of the metallocene catalyst are to: (i) slower the deactivation of the metallocene, (ii) employ less cocatalyst, (iii) protect the reactor fouling, (iv) control the polymer morphologies, and (v) fulfill the requirements of the commercial polymerization processes [1–3]. It has been known that polyethylene, such as the linear low-density polyethylene (LLDPE) can be obtained via the copolymerization of ethylene with various alpha olefins. They have grown significantly due to the specific properties that can be obtained by varying comonomer contents and polymerization conditions.

Polymer nanocomposites have attracted a great deal of interest from material scientists since their applications have dramatically improved material properties in engineering plastics. These characteristics usually arised from the synergistic effect due to the addition of the nanofillers. Depending on the composition and microstructure, the effects of different nanoparticles on the properties of polymers are different. The most commonly used inorganic nanoparticles are SiO_2 [4–7], TiO_2 [8–11], Al_2O_3 [12, 13], and ZrO_2 [14, 15]. In addition, TiO_2 nanoparticles were used as fillers in order to produce new materials. Due to many interesting properties of TiO_2 , such as anti-bacterial with photocatalysis technique (when exposed to light radiation, the pairs of electron-cavity are formed on TiO_2 , and consequently the oxygen and water absorbed on the surface of TiO_2 are radicalized). Hydroxyl (OH) excited by light plays an important role in catalysis reaction. It attacks the microorganisms and makes them lose activity [9] and optical properties (absorption of UV light up to the proximity of visible wavelengths, transparency at visible wavelengths, and very high refractive index) [8]. In general, polymer nanocomposites can be prepared by three methods, such as (i) a melt mixing [16–18], (ii) a solution blending [19], and (iii) in situ polymerization [11, 15, 20]. Due to the direct synthesis via polymerization along with the presence of fillers, the in situ polymerization is perhaps considered the most promising technique to produce polymer nanocomposites with homogeneous distribution of the nanoparticles inside the polymer matrix. Although LLDPE/ TiO_2 nanocomposites have been investigated by some authors [8–10], only the melt mixing or solution blending processes were employed to synthesize those polymer samples.

Based on our work dealing with the use of TiO_2 as the support for cobalt (Co) catalysts, we found that the catalytic behaviors were dependent of the crystalline phases of TiO_2 [21–24]. In this study, we extend our study by investigating the effect of TiO_2 phases coupled with $[\text{Al}]_{\text{dMMMAO}}/[\text{Zr}]_{\text{cat}}$ ratios on the synthesis of LLDPE/ TiO_2 nanocomposites. The catalytic activity and properties of polymer nanocomposites obtained upon different $[\text{Al}]_{\text{dMMMAO}}/[\text{Zr}]_{\text{cat}}$ ratios were further discussed in more details.

Experimental

Materials

All chemicals and polymerization were handled under an argon atmosphere using a glove box and/or Schlenk techniques. The TiO_2 nanoparticles [99.7% of anatase having surface area of $240 \text{ m}^2/\text{g}$ designated as TiO_2 (A) and 99.5% of rutile having surface area of $160 \text{ m}^2/\text{g}$ designated as TiO_2 (R)] were purchased from Aldrich Chemical Company, Inc., and they were heated at 673 K under vacuum for 6 h prior to impregnation with dried MMAO (dMMAO). Toluene was dried over dehydrated CaCl_2 and distilled over sodium/benzophenone before use. The *rac*-ethylenebis(indenyl) zirconium dichloride (*rac*-Et[Ind]₂ZrCl₂) was supplied from Aldrich Chemical Company, Inc. Modified methylaluminoxane (MMAO) in hexane was donated by Tosoh (Akso, Japan). Trimethylaluminum (TMA, 2 M in toluene) was supplied by Nippon Aluminum Alkyls, Ltd., Japan. Ultrahigh purity argon was further purified by passing it through columns that were packed with BASF catalyst R3-11G (molecular-sieved to 3 Å), sodium hydroxide (NaOH), and phosphorus pentaoxide (P₂O₅) to remove traces of oxygen and moisture. Ethylene gas (99.96%) was donated by the National Petrochemical Co., Ltd., Thailand. 1-Hexene (99+, *d* = 0.673 g/mL) was purchased from Aldrich Chemical Company, Inc.

Preparation of dried MMAO

Removal of TMA from MMAO was carried out according to the reported procedure [25]. The toluene solution of MMAO was dried under vacuum for 6 h at room temperature to evaporate the solvent, TMA and TIBA. Then, continue to dissolve with 100 mL of heptane and the solution was evaporated under vacuum to remove the remaining TMA and TIBA. This procedure was repeated four times and the white powder of dMMAO was obtained. Based on this technique, about 40% of TMA can be removed [25].

Preparation of dMMAO impregnated on TiO_2 nanoparticles (dMMAO/ TiO_2)

The dMMAO (1.00 g or 16.3 mmol) was impregnated on TiO_2 (1.30 g or 12.5 mmol) in 20 mL of toluene at room temperature. The mixture was stirred for 30 min. The solvent was then removed from the mixture by evacuation. This procedure was done only once with toluene (20 mL × 1) and thrice with hexane (20 mL × 3). Then, the solid part was evaporated and dried under vacuum at room temperature. The white powder of dMMAO/ TiO_2 was then obtained.

Polymerization reaction

The copolymerization of ethylene/1-hexene was carried out in a 100 mL semi-batch stainless steel autoclave reactor equipped with magnetic stirrer. In the glove box, the desired amount of *rac*-Et[Ind]₂ZrCl₂ and TMA was mixed and stirred for 5 min

aging to affect alkylation of the zirconocene catalyst. Then, toluene (to make a total volume of 30 mL) and desired amounts of dMMAO/TiO₂ corresponding to the [Al]_{dMMAO}/[Zr]_{cat} ratios of 1135, 2270, and 3405 were introduced into the reactor for each run. In addition, the amount of [Al]_{dMMAO} present on each dMMAO/TiO₂ sample was determined by energy dispersive X-ray spectroscopy (EDX). After that the mixture of *rac*-Et[Ind]₂ZrCl₂ and TMA was injected into the reactor. The reactor was frozen in liquid nitrogen to stop reaction and then 0.018 mol of 1-hexene was injected into the reactor. The autoclave was evacuated to remove the argon. Then, the reactor was heated up to polymerization temperature (343 K) and the polymerization was started by feeding ethylene gas (total pressure 50 psi in the reactor) until the consumption of ethylene at 0.018 mol (decreased ethylene pressure of 6 psi was observed) was reached. The reaction of polymerization was terminated by addition of acidic methanol (0.1% HCl in methanol). The reaction time was recorded for purpose of calculating the activity. The precipitated polymer was washed with methanol and dried at room temperature.

Characterization procedures

Characterization of the TiO₂ nanofillers and catalyst precursor

X-ray diffraction: XRD was performed to determine the bulk crystalline phases of samples. It was conducted using a SIEMEN D-5000 X-ray diffractometer with Cu K α ($\lambda = 1.54439 \text{ \AA}$). The spectra were scanned at a rate of 2.4°/min in the range $2\theta = 20\text{--}80^\circ$.

Transmission electron microscopy: TEM was used to determine the shape and crystalline size of TiO₂ nanoparticles. The sample was dispersed in ethanol prior to TEM measurement using TEM (JEOL JEM-2010) for microstructural characterization.

Thermal gravimetric analysis: TGA was performed using a TA Instruments SDT Q-600 analyzer. The samples of 10–20 mg and a temperature ramping from 298 to 873 K at 2 K/min were used in the operation. The carrier gas was N₂ UHP.

Scanning electron microscopy and energy dispersive X-ray spectroscopy: SEM and EDX were used to investigate the sample morphologies and elemental distribution throughout the nanofillers. The SEM of JEOL mode JSM-5800 LV scanning microscope was employed. EDX was further performed using Link Isis series 300 program.

Characterization of polymer

Transmission electron microscopy: TEM was used to determine the dispersion of TiO₂ nanofillers in LLDPE. The same equipment as mentioned before was employed.

¹³C NMR spectroscopy: ¹³C NMR spectroscopy was used to determine the 1-hexene incorporation and copolymer microstructure. Chemical shifts were referenced internally to the CDCl₃ and calculated according to the method described by Randall [26]. Each sample solution was prepared by dissolving 50 mg of copolymer in 1,2-dichlorobenzene and CDCl₃. The ¹³C NMR spectra were taken

at 373 K using a BRUKER AVANCE II 400 operating at 100 MHz with an acquisition time of 1.5 s and delay time of 4 s.

Results and discussion

In this study, the synthesis of LLDPE/TiO₂ nanocomposites using the TiO₂ nanoparticles having different crystalline phases and ratios of [Al]_{dMMAO}/[Zr]_{cat} with zirconocene/dMMAO catalyst for ethylene/1-hexene copolymerization was investigated. First, the TiO₂ nanoparticles before and after impregnation with dMMAO were characterized using different techniques. The XRD patterns of samples are shown in Fig. 1 indicating the characteristic peaks for the anatase form of TiO₂ (A) at 25° (major), 38°, 48°, 55°, and 63° and the rutile form of TiO₂ (R) at 27° (major), 36°, 41°, and 54°. Average crystallite sizes for both TiO₂ (A) and TiO₂ (R) was calculated from the major peaks obtained from XRD using Sherrer's equation. It was found that the average crystallite sizes of TiO₂ (A) and TiO₂ (R) were 6.1 and 6.9 nm, respectively. After impregnation with dMMAO, the XRD patterns for both samples apparently exhibited the similar patterns as seen before impregnation with dMMAO. On the other hand, no peaks of dMMAO were detected. This was suggested that the dMMAO was present in the highly dispersed form on the TiO₂ nanoparticles after impregnation.

The SEM micrographs and EDX mapping for the dMMAO/TiO₂ samples (not shown) revealed the similar morphologies. It can be observed that the dMMAO was well-distributed all over the TiO₂ granules as seen by the EDX mapping. Based on the EDX measurement, the amounts of [Al]_{dMMAO} present on the TiO₂ samples can be determined. They were within the range of 12.5 and 10.2 wt% for TiO₂ (A) and TiO₂ (R), respectively. The larger amount of [Al]_{dMMAO} present in the TiO₂ (A) can be attributed to larger surface area for the TiO₂ (A) resulting in better dispersion of

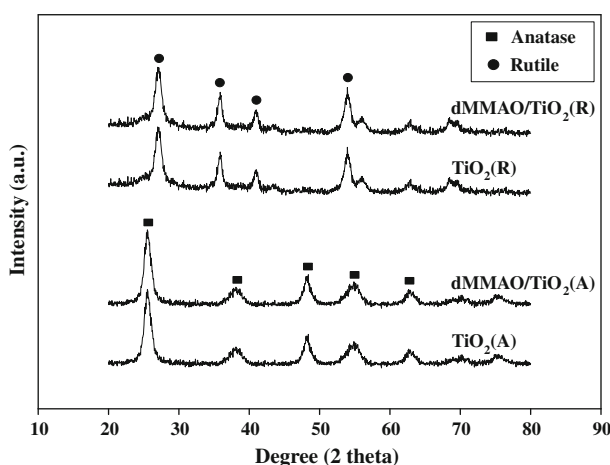


Fig. 1 XRD patterns of different TiO₂ nanoparticles before and after impregnation with dMMAO

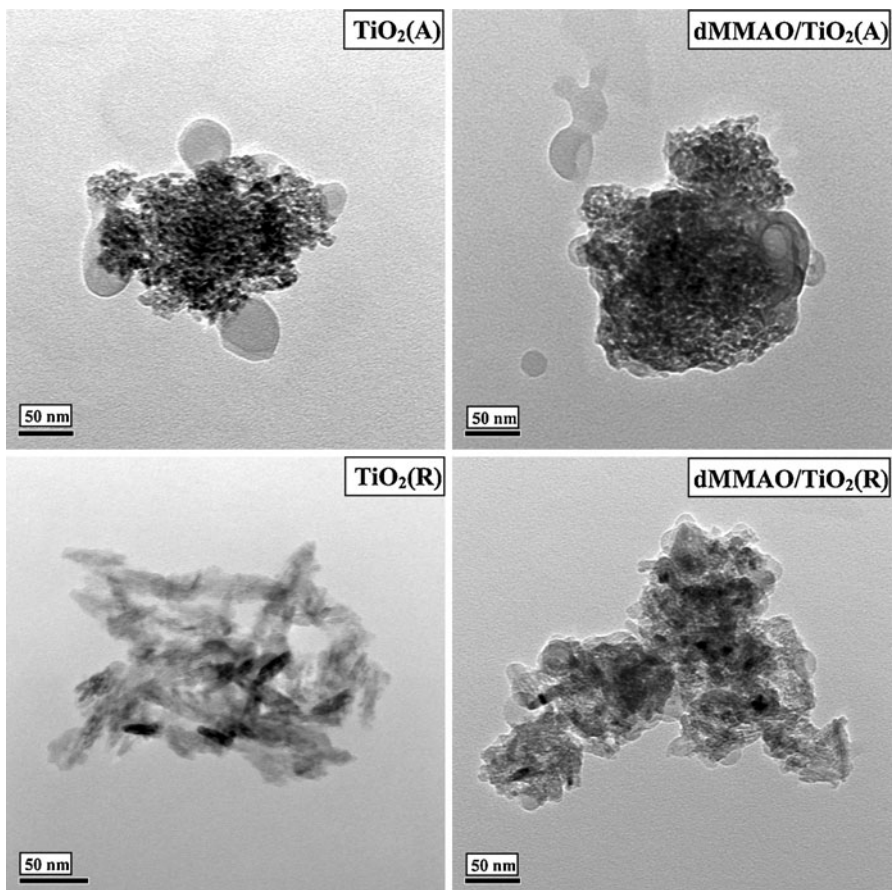


Fig. 2 TEM micrographs of different TiO₂ nanoparticles before and after impregnation with dMMAO

dMMAO on the TiO₂ (A) nanofiller. The TEM micrographs of both TiO₂ nanoparticles before and after impregnation with dMMAO are also shown in Fig. 2. It indicated that the TiO₂ (A) crystals appeared in the spherical-like shape, whereas the TiO₂ (R) crystals were in the needle-like shape. It appeared that the crystalline size of primary particle obtained from the TEM measurement was below 50 nm for both samples, as seen in Fig. 2. In addition, the crystalline sizes for both TiO₂ samples became larger after impregnation with dMMAO due to the deposition of dMMAO on the TiO₂ nanofillers.

Then, the in situ polymerization of ethylene/1-hexene was performed with the presence of dMMAO/TiO₂ using zirconocene catalyst to produce the LLDPE/TiO₂ nanocomposites. The amounts of dMMAO/TiO₂ employed were varied based on the amounts of [Al]_{dMMAO}/[Zr]_{cat} being present as determined by EDX measurement to keep the [Al]_{dMMAO}/[Zr]_{cat} ratios at 1135, 2270, and 3405 for both TiO₂ (A) and TiO₂ (R). Thus, the catalytic activity can be compared with regards to the identical [Al]_{dMMAO}/[Zr]_{cat} ratios. The resulted catalytic activities obtained from both

Table 1 Polymerization activities of LLDPE/TiO₂ nanocomposites synthesized by in situ polymerization with *rac*-Et(Ind)₂ZrCl₂/dMMAO catalysts

Types of filler	[Al] _{dMMAO} /[Zr] _{cat}	Time ^a (s)	Polymer yield ^b (g)	Catalytic activity (kg pol./mol Zr h)	Relative activity ^c
TiO ₂ (A)	1135	229	0.91	9,564	1
	2270	171	1.01	14,123	1.5
	3405	133	1.13	20,403	2.1
TiO ₂ (R)	1135	345	0.30	2,098	1
	2270	266	0.41	3,667	1.7
	3405	234	0.59	6,100	2.9

^a A period of time used for the total 0.018 mol of ethylene to be consumed

^b Measurement at polymerization temperature of 343 K, [Ethylene] = 0.018 mol, [Al]_{TMA}/[Zr]_{cat} = 2500, in toluene with total volume = 30 mL, and [Zr]_{cat} = 5 × 10⁻⁵ M

^c Relative activity was calculated based on increased activity compared to the activity obtained with [Al]_{dMMAO}/[Zr]_{cat} = 1135 for the same filler

dMMAO/TiO₂ (A) and dMMAO/TiO₂ (R) with different ratios of [Al]_{dMMAO}/[Zr]_{cat} are summarized in Table 1. It was found that the dMMAO/TiO₂ (A) sample exhibited about four times higher activities than those obtained from the dMMAO/TiO₂ (R) sample upon the same [Al]_{dMMAO}/[Zr]_{cat} ratios. This was likely due to higher intrinsic activity of the active species based on [Al]_{dMMAO} present on the TiO₂ (A) [11]. In addition, increased [Al]_{dMMAO}/[Zr]_{cat} ratios also resulted in increased activities for both dMMAO/TiO₂ (A) and dMMAO/TiO₂ (R). This indicated that the greater amounts of dMMAO can be responsible for increased active species being present during polymerization. It was proposed that the alkylaluminum as a cocatalyst possibly had many functions, such as an alkylating agent, a stabilizer for a cationic metallocene alkyl, and/or counter-ion, an ionizing and/or reducing agent for the transition element, and a scavenger for the metallocene catalytic system. However, one of the most important roles of this alkylaluminoxane is apparently to prevent the formation of ZrCH₂CH₂Zr species, which is formed via a bimolecular process [13]. Considering the increase of activity upon increased [Al]_{dMMAO}/[Zr]_{cat} ratios, a plot of the relative activity versus [Al]_{dMMAO}/[Zr]_{cat} ratios is illustrated in Fig. 3 for better understanding. Here, the term of theoretical relative activity is given to describe an increase in activity with increased amount of [Al]_{dMMAO} as a cocatalyst or activator. As a matter of fact, increased amount of the activator would result in increased active sites as a linear relationship theoretically, which is essentially not true due to the deactivation of active sites. Based on the definition, it can be expected that the theoretical relative activity would increase two or three times with increased [Al]_{dMMAO}/[Zr]_{cat} ratios at two or three times, respectively. However, it can be observed that the relative activity for both TiO₂ (A) and TiO₂ (R) was lower than the theoretical value. This was suggested that the deactivation of active sites essentially occurred with increased [Al]_{dMMAO}/[Zr]_{cat} ratios. It should be mentioned that the TiO₂ (R) exhibited less deactivation than the TiO₂ (A) due to higher relative activity as seen in Fig. 3. This can be caused by different interaction as proven by the TGA measurement.

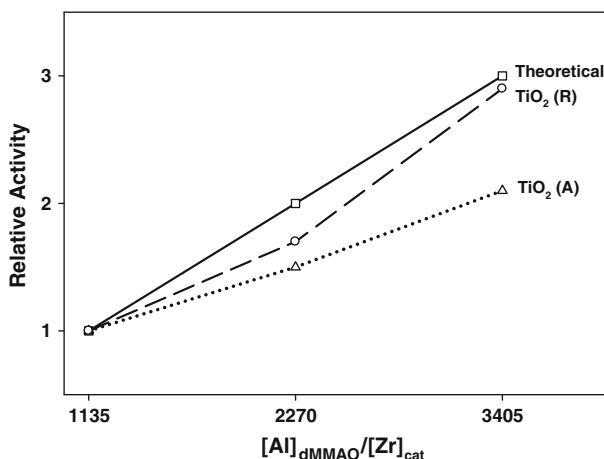


Fig. 3 Relative activity of TiO₂ at different [A]_{dMMAO}/[Zr]_{cat} ratio

Besides the difference in intrinsic activity, the interactions between the [Al]_{dMMAO} and TiO₂ nanoparticles is also a key factor to consider. In fact, the strong interaction of the active species with TiO₂ nanoparticles employed in this study was essentially referred to the interactions between the TiO₂ nanoparticles and the dMMAO cocatalyst. Based on this study, the dMMAO was impregnated onto the TiO₂ nanoparticles prior to polymerization. The degree of interactions between the TiO₂ nanoparticles and dMMAO can be determined by the TGA measurement. In order to give a better understanding, we propose the interactions of TiO₂ nanoparticles and dMMAO based on the review paper by Severn et al. [27]. They explained that the connection of the nanofiller and cocatalyst occurred via the O_{filler}–Al_{cocatalyst} linkage. In particular, the TGA can only provide useful information on the degree of interactions for the dMMAO bound to the TiO₂ nanoparticles in terms of the weight loss and removal temperature. The stronger interaction can result in it being more difficult for the dMMAO bound to the TiO₂ nanoparticles to react with Zr-complex during activation processes, leading to lower catalytic activity for polymerization [28]. The TGA measurement was performed to prove the interaction between the [Al]_{dMMAO} and TiO₂ nanoparticles. The TGA profiles of both dMMAO/TiO₂ samples are given in Fig. 4. The decomposition temperature (T_d) at 10% weight loss of [Al]_{dMMAO} present on TiO₂ nanoparticles was at 455 and 470 K for TiO₂ (A) and TiO₂ (R), respectively. This indicated that the dMMAO stronger interacted with the TiO₂ (R) sample resulting in the higher decomposition temperature. Based on the TGA measurement, the higher relative activity obtained from the TiO₂ (R) can be attributed to stronger interaction resulting in less deactivation as mentioned earlier.

It would be interesting to disclose how different crystalline phases of TiO₂ can affect the polymer properties. Thus, the LLDPE/TiO₂ nanocomposites obtained were further characterized by means of TEM and ¹³C NMR. As known, the images from high-resolution transmission electron microscopy (TEM) are essential components of nanoscience and nanotechnology, therefore TEM was performed to determine the

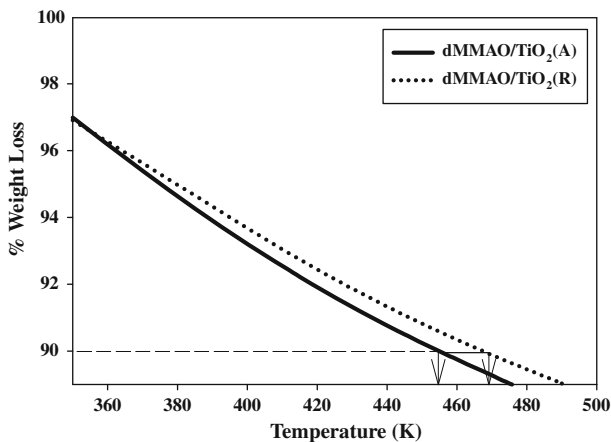


Fig. 4 TGA profiles of $[Al]_{dMMAO}$ on different TiO_2 nanoparticles

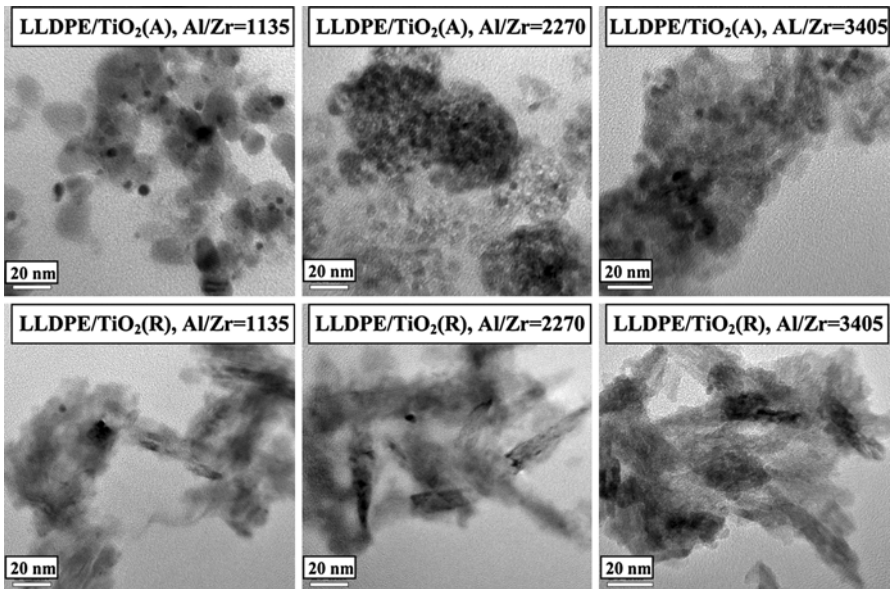


Fig. 5 TEM micrographs of both LLDPE/TiO₂ (A) and LLDPE/TiO₂ (R) nanocomposites having different $[Al]_{dMMAO}/[Zr]_{cat}$ ratios

dispersion of TiO_2 nanoparticles inside the polymer matrix. The TEM micrographs for the dispersion of TiO_2 in the LLDPE/TiO₂ (A) and LLDPE/TiO₂ (R) nanocomposites having different $[Al]_{dMMAO}/[Zr]_{cat}$ ratios are shown in Fig. 5. In general, both TiO_2 (A) and TiO_2 (R) nanoparticles apparently exhibited good dispersion inside the polymer matrix without any changes in crystal morphologies.

The ^{13}C NMR is one of the most powerful techniques used to identify the polymer microstructure, especially for polyolefins. The resulted ^{13}C NMR spectra

Table 2 ^{13}C NMR analysis of LLDPE/TiO₂ nanocomposites

Types of filler	[Al] _{dMMAO} /[Zr] _{cat}	EEE	HEE	EHE	EHH	HEH	HHH	%H
TiO ₂ (A)	1135	0.546	0.210	0.127	0.080	0.036	0.000	21
	2270	0.464	0.185	0.169	0.126	0.056	0.000	29
	3405	0.447	0.231	0.141	0.133	0.048	0.000	27
TiO ₂ (R)	1135	0.825	0.119	0.056	0.000	0.000	0.000	6
	2270	0.747	0.168	0.079	0.007	0.000	0.000	8
	3405	0.757	0.159	0.079	0.005	0.000	0.000	8

E refers to ethylene and H refers to 1-hexene

(not shown) for all samples were assigned typically to the LLDPE obtained from copolymerization of ethylene/1-hexene. The triad distribution was identified based on the method described by Randall [26]. It can be observed that the LLDPE/TiO₂ (A) and LLDPE/TiO₂ (R) nanocomposites exhibited similar ^{13}C NMR patterns indicating similar molecular structure of polymer. Based on calculations described by Galland [29], the triad distribution of monomer is listed in Table 2. It indicated that all LLDPE/TiO₂ nanocomposites obtained were random copolymer with differences in triad distribution. This is the nature of zirconocene catalyst used in this study as reported on our previous studies [6, 7, 11, 30]. It should be mentioned that the LLDPE/TiO₂ (R) nanocomposites exhibited lower %H insertion (<10%) probably due to more steric hindrance.

Summary

The catalytic activity is dependent on the crystalline phases of TiO₂ for the LLDPE/TiO₂ nanocomposites produced via in situ polymerization of ethylene/1-hexene with zirconocene/dMMAO catalyst. The dMMAO/TiO₂ (A) exhibited about four times higher intrinsic activity based on dMMAO than the dMMAO/TiO₂ (R). However, the dMMAO/TiO₂ (R) showed higher relative activity with increased [Al]_{dMMAO}/[Zr]_{cat} ratios suggesting less deactivation of catalytic sites. This can be attributed to stronger interaction between dMMAO and TiO₂ (R). No significant changes on the polymer microstructure were found upon different crystalline phases of TiO₂. However, the LLDPE/TiO₂ (R) nanocomposites rendered lower %H insertion.

Acknowledgments We thank the Thailand Research Fund (TRF) under DBG52-B. Jongsomjit project.

References

1. Turunen JPL, Pakkanen TT (2007) Characterization of stepwise prepared, silica supported zirconocene catalysts designed for olefin polymerization. *J Mol Catal A* 263:1–8
2. Ribeiro MR, Deffieux A, Portela MF (1997) Supported metallocene complexes for ethylene and propylene polymerizations: preparation and activity. *Ind Eng Chem Res* 36:1224–1237

3. Chien JCW (1999) Supported metallocene polymerization catalysis. *Top Catal* 7:23–36
4. Kontou E, Niaounakis M (2006) Thermo-mechanical properties of LLDPE/SiO₂ nanocomposites. *Polymer* 47:1267–1280
5. Li KT, Dai CL, Kuo CW (2007) Ethylene polymerization over a nano-sized silica supported Cp₂ZrCl₂/MAO catalyst. *Catal Commun* 8:1209–1213
6. Jongsomjit B, Chaichana E, Praserthdam P (2005) LLDPE/nano-silica composites synthesized via in situ polymerization of ethylene/1-hexene with MAO/metallocene catalyst. *J Mater Sci* 40:2043–2045
7. Chaichana E, Jongsomjit B, Praserthdam P (2007) Effect of nano-SiO₂ particle size on the formation of LLDPE-SiO₂ nanocomposite synthesized via in situ polymerization with metallocene catalyst. *Chem Eng Sci* 62:899–905
8. Nussbaumer RJ, Caseri WR, Tervoort PT (2003) Polymer-TiO₂ nanocomposites: a route towards visually transparent broadband UV filters and high refractive index materials. *Macromol Mater Eng* 288:44–49
9. Wang Z, Li G, Xie G, Zhang Z (2005) Dispersion behavior of TiO₂ nanoparticles in LLDPE/LDPE/TiO₂ nanocomposites. *Macromol Chem Phys* 206:258–262
10. Chen XD, Wang Z, Liao ZF, Mai YL, Zhang MQ (2007) Roles of anatase and rutile TiO₂ nanoparticles in photooxidation of polyurethane. *Polym Test* 26:202–208
11. Owpradit W, Jongsomjit B (2008) A comparative study on synthesis of LLDPE/TiO₂ nanocomposites using different TiO₂ by in situ polymerization with zirconocene/dMMAO catalyst. *Mater Chem Phys* 112:954–961
12. Kuo MC, Tsai CM, Huang JC, Chen M (2005) PEEK composites reinforced by nano-sized SiO₂ and Al₂O₃ particulates. *Mater Chem Phys* 90:185–195
13. Desharun C, Jongsomjit B, Praserthdam P (2008) Study of LLDPE/alumina nanocomposites synthesized by in situ polymerization with zirconocene/d-MMAO catalyst. *Catal Commun* 9:522–528
14. Jongsomjit B, Panpranot J, Okada M, Shiono T, Praserthdam P (2006) Characteristics of LLDPE/ZrO₂ nanocomposite synthesized by the in situ polymerization using a zirconocene/MAO catalyst. *Iran Polym J* 15:431–437
15. Jongsomjit B, Panpranot J, Praserthdam P (2007) Effect of nanoscale SiO₂ and ZrO₂ as the fillers on the microstructure of LLDPE nanocomposites synthesized via in situ polymerization with zirconocene. *Mater Lett* 61:1376–1379
16. Nawang R, Danajai ID, Ishiaku US, Ismail H, Ishak ZAM (2001) Mechanical properties of sago starch-filled linear low density polyethylene (LLDPE) composites. *Polym Test* 20:167–172
17. Verbeek CJR (2002) Highly filled polyethylene/phlogopite composites. *Mater Lett* 52:453–457
18. Huang YQ, Zhang YQ, Hua YQ (2003) Studies on dynamic mechanical and rheological properties of LLDPE/nano-SiO₂ composites. *J Mater Sci Lett* 22:997–998
19. Rossi GB, Beaucage G, Dang TD, Vaia RA (2002) Bottom-up synthesis of polymer nanocomposites and molecular composites: ionic exchange with PMMA latex. *Nano Lett* 2:319–323
20. Cheng W, Wang Z, Ren R, Chen H, Tang T (2007) Preparation of silica/polyacrylamide/polyethylene nanocomposite via in situ polymerization. *Mater Lett* 61:3193–3196
21. Jongsomjit B, Sakdammuson C, Praserthdam P (2005) Dependence of crystalline phases in titania on catalytic properties during CO hydrogenation of Co/TiO₂ catalysts. *Mater Chem Phys* 89:395–401
22. Jongsomjit B, Wongsalee T, Praserthdam P (2005) Study of cobalt dispersion on titania consisting various rutile:anatase ratios. *Mater Chem Phys* 92:572–577
23. Jongsomjit B, Wongsalee T, Praserthdam P (2005) Characteristics and catalytic properties of Co/TiO₂ for various rutile:anatase ratios. *Catal Commun* 6:705–710
24. Wongsalee T, Jongsomjit B, Praserthdam P (2006) Effect of zirconia-modified titania consisting of different phases on characteristics and catalytic properties of Co/TiO₂ catalysts. *Catal Lett* 108:55–61
25. Hagimoto H, Shiono T, Ikeda T (2004) Supporting effects of methylaluminoxane on the living polymerization of propylene with a chelating (diamide)dimethyltin complex. *Macromol Chem Phys* 205:19–26
26. Randall JC (1989) A review of high resolution liquid ¹³C NMR characterizations of ethylene-based polymer. *J Macromol Sci Rev Macromol Chem Phys C* 29:201–315
27. Sevem JR, Chadwick JC, Duchateau R, Frienderichs N (2005) “Bound but not gagged”: immobilizing single-site α -olefin polymerization catalysts. *Chem Rev* 105:4073–4147
28. Ketloy C, Jongsomjit B, Praserthdam P (2007) Characteristics and catalytic properties of [t-BuN-SiMe₂Flu]TiMe₂/dMMAO catalyst dispersed on various supports towards ethylene/1-octene copolymerization. *Appl Catal A* 327:270–277

29. Galland GB, Quijada P, Mawler RS, de Menezes SC (1996) Determination of reactivity ratios for ethylene/ α -olefin copolymerization catalysed by the $C_2H_4[Ind]_2ZrCl_2$ /methylaluminoxane system. *Macromol Rap Commun* 17:607–613
30. Jongsomjit B, Kaewkrajang P, Shiono T, Praserthdam (2004) Supporting effects of silica-supported MAO with zirconocene catalyst on ethylene/1-olefin copolymerization behaviors for LLDPE production. *Ind Eng Chem Res* 43:7959–7963